ACS OMEGA

http://pubs.acs.org/journal/acsodf

Article

Probing Adaptation of Hydration and Protein Dynamics to Temperature

Luan C. Doan, Jayangika N. Dahanayake, Katie R. Mitchell-Koch, Abhishek K. Singh, and Nguyen Q. Vinh*

Cite This: *ACS Omega* 2022, 7, 22020−22031

Read Online

ACCESS | Metrics & More | Article Recommendations | Supporting Information

ABSTRACT: Protein dynamics is strongly influenced by the surrounding environment and physiological conditions. Here we employ broadband megahertz-to-terahertz spectroscopy to explore the dynamics of water and myoglobin protein on an extended time scale from femto- to nanosecond. The dielectric spectra reveal several relaxations corresponding to the orientational polarization mechanism, including the dynamics of loosely bound, tightly bound, and bulk water, as well as collective vibrational modes of protein in an aqueous environment. The dynamics of loosely bound and bulk water follow non-Arrhenius behavior; however, the dynamics of water molecules in the tightly bound layer obeys the Arrhenius-type relation. Combining molecular simulations and effective-medium approximation, we have determined the number of water molecules in the tightly bound hydration layer and studied the dynamics of protein as a function of temperature. The results provide the important impact of water on the biochemical functions of proteins.

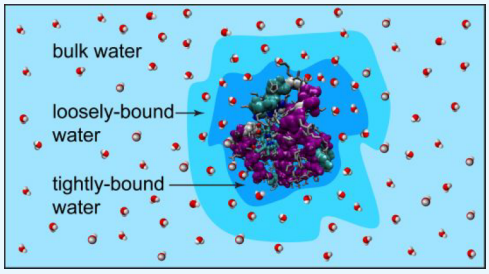

1. INTRODUCTION

Protein function is strongly dependent on protein flexibility and stability in aqueous environments.[1−9] The relationship between structure and function is assumed to be optimized with respect to proteins' physiological conditions. Our knowledge of the dynamics of proteins and their environments' contributions to biochemical and molecular mechanisms falls behind our understanding of three-dimensional structures and biological mechanisms.[1,6,8,10,11] This is due to a wide range of internal motions, the complexity of protein systems, and their environments, including the solvent and temperature.[12,13] Water is an important solvent for the functionality of proteins. Water is present in hydration shells around proteins and beyond these layers in the bulk form. The dynamics of water and protein, as well as protein−water interactions, are strongly sensitive to temperature. At physiological temperatures, protein must maintain specific three-dimensional conformations required for biochemical functions, e.g., for recognizing and binding ligands. The structural stability of protein must not be so substantial as to interfere with the precise and rapid variations in structure during catalysis, binding, and metabolic regulation. Thus, the stability and flexibility of proteins need to be in balance at physiological temperatures.

Water at the interface between protein and bulk water is essential for the protein's stability and flexibility. Thus, to understand the biological functions of proteins, the dynamics and structure of the interfacial or hydration water molecules need to be explored. It is well documented that hydration water molecules covering protein surfaces do not freeze until the temperature is well below the crystal homogeneous nucleation point ($T_h \sim 235$ K), an important property for biological functioning.[13,14] The dynamics of hydration water as well as hydrated proteins connects to their glass transition temperature.[15,16] It is generally accepted that the local changes of protein are slaved by the dynamics of water in the first hydration shell (δ_1-relaxation), whereas the global conformational motions are driven by all water molecules around the protein, including water in hydration shells (δ_1-, δ_2-relaxation) and bulk water (γ-relaxation).[8,10,17] Note that different processes are labeled following the biophysical nomenclature, in which the δ-relaxations of hydration water correspond to the β-relaxations, the γ-relaxation of bulk water is regarded as the α-relaxation in the glass-physics classification, and β-relaxation denotes the tumbling of dipolar biomolecules in solution.[8,11] The δ-relaxations of hydration water are located between γ- and β-relaxations. It has been suggested that the dynamics crossover in the orientational time of water molecules (from non-Arrhenius to Arrhenius behavior) could be related to the anomalies of water, but it is independent of liquid−liquid critical point.[18] Also, an understanding of dynamics and structure of water in the intermediate region (δ_2-relaxation)

Received: May 7, 2022
Accepted: May 31, 2022
Published: June 13, 2022

between the first hydration shell (δ_1-relaxation) and bulk water (γ-relaxation) is still incomplete.

The dynamics of proteins and surrounding water molecules must be thermally driven; thus, the stability and flexibility of hydrated proteins are strongly dependent on the temperature. Molecular adaptation to the change in temperature seems to be accompanied by altered dynamics and structure of water molecules around proteins.[19] Thus, in view of protein thermal stability, the dynamics of proteins and hydration layers have an optimum temperature at which they have evolved. Several studies based on molecular dynamics (MD) simulations have recently probed the critical dynamics taking place at biomolecular interfaces and the effect of temperature variation.[20−25] The dielectric spectra from megahertz to terahertz frequencies of aqueous protein solutions reveal several dispersion regions,[7,8,10] including the typical signatures of relaxation processes of bound and bulk water as well as the collective motions of proteins in solutions. Careful analysis of the dynamics of water and protein in solution over an extended range of temperature allows us to understand protein−water interactions and the flexibility of proteins, which is maintained at varying temperatures. We focus on the dielectric response of both relaxation processes and collective motions of myoglobin solutions at different temperatures in the present work.

2. EXPERIMENTAL METHODS

2.1. Sample Preparation. Myoglobin solutions were prepared by measuring and weighing protein and determining the volume of protein solutions after dissolving myoglobin protein in pure water. Myoglobin protein obtained from Sigma-Aldrich (Cat. No. M0630) with a molecular weight of 17.0 kDa was used to prepare myoglobin solutions. To accurately determine the volume filling factor of the protein, f_p, and the molar concentrations, myoglobin protein was dissolved in 10 mL of deionized water (resistivity of ∼18 MΩ cm) in a volumetric flask. The measurement accuracy is ±0.03 mL or 0.5%. The dielectric response of the myoglobin solutions was determined accurately from 200 MHz to 1.12 THz with protein concentration from micromolar to millimolar using a megahertz-to-terahertz frequency-domain spectrometer based on a vector network analyzer.[26−32]

2.2. Dielectric Spectroscopy. To explore the temperature effect on hydration dynamics and structure along with collective motions of biomolecules in aqueous environment, we have employed a frequency-domain dielectric spectrometer covering the spectral range from 200 MHz to 1.12 THz (0.00667−37.36 cm^{-1}).[26−28,31,32] The spectrometer consists of two main parts, including a dielectric probe and frequency extenders together with a vector network analyzer. A dielectric probe (HP 85070E) has been used to characterize the low frequency dielectric response from 200 MHz to 50 GHz. The dielectric response of a solution at the terahertz frequency has been collected using frequency extenders from Virginia Diodes, with the frequency spanning a wide range from 60 GHz to 1.12 THz. To overcome the strong absorption of water, we have developed the spectrometer to achieve a high dynamical range up to 120 dB and simultaneously obtain intensity and phase information on aqueous solutions.[26] To ensure the thermal stability of the solutions, we built a sample cell with anodized aluminum and a variable optical path length for dielectric measurements. Two transparent parallel windows at the terahertz frequencies were installed inside the sample cell, in which one is fixed and the other is in a mobile position with submicrometer precision (∼0.08 μm). To control the temperature, we cooled the sample cell with Peltier coolers (Custom Thermoelectric) and heated it with power resistors inserted in the cell. The temperature was monitored and controlled with an accuracy of ±0.02 °C, using a temperature controller (Lakeshore 336). From the phase and intensity results as a function of the sample thickness, we have determined the refractive index and absorption of solutions at each frequency. The variable optical path-length cell combined with the high dynamic range of the terahertz spectrometer allows us to obtain the most precise and accurate megahertz-to-terahertz dielectric spectra reported so far for this frequency region.

2.3. Molecular Dynamics Simulations. The starting coordinates for simulations of deoxy myoglobin protein were taken from the X-ray crystallographic structure (PDB ID: 1bzp).[33] Crystallographic water molecules were kept with protein to achieve fast equilibration in the aqueous simulation.[34] MD simulations were performed using *GROMACS* (version 2019.5)[35] software package. *CHARMM36* force field[36] was used for the protein, and the SPC/E water model was used to represent water. The SPC/E model[37] has shown the best reproduction of experimental water reorientation times and diffusion compared to the other common, simple, fixed charge water force field models.[38] For the MD simulations, six temperatures were considered: 278, 288, 298, 308, 318, and 328 K.

The protein was centered in a cubic periodic box with a minimum distance of 1.0 nm between protein and any side of the box, and then the protein was solvated with water. In order to neutralize the systems at a 0.15 M salt concentration, Na^+ and Cl^- ions were added. As the bond length constraint, Linear Constraint Solver (LINCS) algorithm was used and for electrostatic interactions,[39] particle mesh Ewald summation was used.[40] For long-range interactions, grid spacing of 0.12 nm combined with an interpolation order of 4 was used. For van der Waals interactions, a cutoff value of 0.4 nm was used. Energy minimization was performed using steepest descent algorithm. Annealing step was carried out by gradually heating the system from 50 K to the desired temperature, throughout a time period of 200 ps. Position restraints were imposed on heavy atoms during the annealing step. Each system was equilibrated in the NPT ensemble for 20 ns at each temperature using V-rescale thermostat[41] and at 1 bar using Berendsen barostat.[42] Then the production runs were carried out in NVT ensembles at each temperature using Nosé−Hoover thermostat for a canonical ensemble.[43] Results were obtained from sets of 100 ns simulations and three trajectories were generated for each temperature using different randomly assigned initial velocities.

All the analysis calculations were carried out using the *GROMACS* software package. Solvation shells around the protein were selected with cutoff values of 3.5, 4.5 and 9 Å, which were selected according to the water radial distribution function. Rotational autocorrelation functions were calculated using the dipole reorientational autocorrelation function, $C_1(t)$ calculations, determined with *GROMACS* software. Analysis calculations were block-averaged with 25 ns time blocks acquired from multiple trajectories. The terahertz spectra were calculated from MD simulations through density of states (DoS) calculations, which were obtained from the velocity autocorrelation function.

https://doi.org/10.1021/acsomega.2c02843
ACS Omega 2022, 7, 22020−22031

3. RESULTS AND DISCUSSION

The high sensitivity of the megahertz-to-terahertz spectrometer allows us to investigate the dynamics of biomolecules in aqueous solutions.[26] The absorption coefficient and refractive index of myoglobin solutions and pure water at 25 °C as a function of frequency are shown in Figure 1a. The absorption coefficient increases monotonically with frequency, whereas the refractive index gently decreases. Comparing water and myoglobin solutions, both absorption coefficient and refractive index of the myoglobin solutions are lower than those of pure water. This indicates that the presence of myoglobin in water changes the optical properties of the solution. The biomolecules displace position of water molecules, reducing the number of water molecules in the solution. The absorption of biomolecules is lower than that of water at the probed frequencies, thus, the absorption of the solutions is reduced. In addition, water molecules form hydration layers around biomolecules because of the interaction with the protein surface. These water molecules have a strong hydrogen bond with the surface and relax with a longer time constant than that of bulk water.

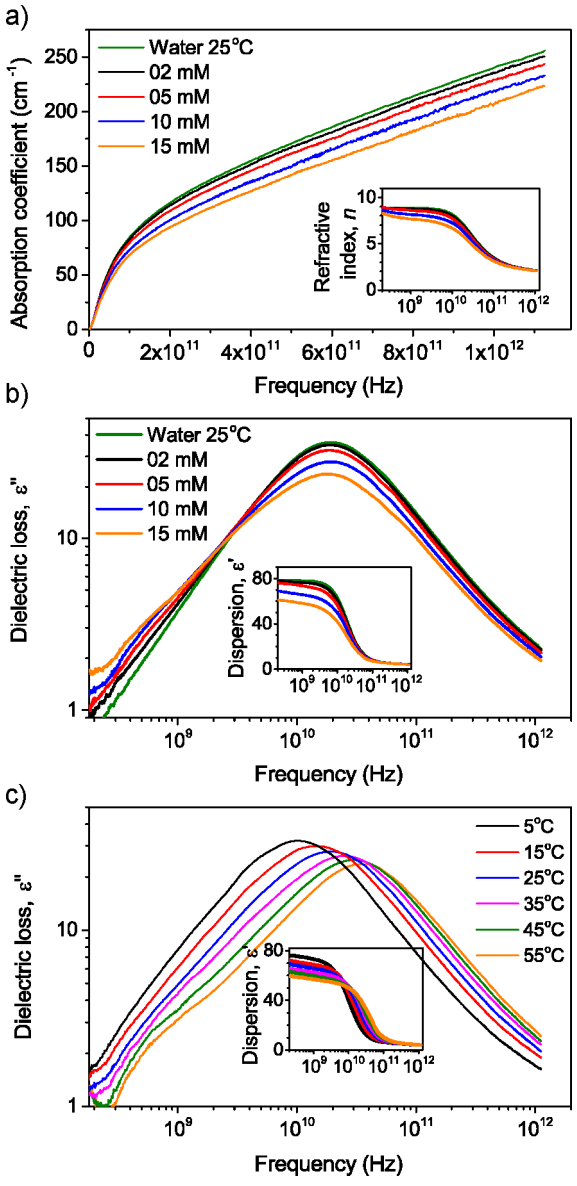

Figure 1. Interaction between aqueous myoglobin solutions and electromagnetic wave in the megahertz to terahertz frequencies revealing the dynamics of water molecules and collective motions of protein in the solutions. (a) Absorption and refractive index (inset) spectra of aqueous myoglobin solutions and pure water increase and decrease with rising frequency, respectively, at 25 °C. (b) Complex dielectric response including dielectric loss and dielectric dispersion (inset) spectra of aqueous myoglobin solutions at 25 °C has been obtained from the absorption and refractive index spectra. (c) Complex dielectric response including dielectric loss and dielectric dispersion (inset) spectra of the 10 mM myoglobin solution has been collected at different temperatures.

The absorption and refractive index as a function of frequency, ν, measured from our setup can be used to calculate the complex index of refraction, $n^*(\nu)$, of a solution:

$$n^*(\nu) = n(\nu) + i\kappa(\nu) \quad (1)$$

where $n(\nu)$ is refractive index, $\kappa(\nu)$ is the extinction coefficient, which is calculated from the absorption coefficient, $\alpha(\nu)$, by $\kappa(\nu) = \alpha(\nu)\bullet c/(4\pi\nu)$ with c being the speed of light. It is convenient to present the complex index of refraction in the form of the dielectric constant, $n^*(\nu) = \sqrt{\varepsilon^*(\nu)}$, of the solution:

$$\varepsilon^*(\nu) = \varepsilon'(\nu) + i\varepsilon''(\nu) + i\sigma/(2\pi\nu\varepsilon_0) \quad (2)$$

where $\varepsilon'(\nu)$ and $\varepsilon''(\nu)$ are the real part (or dielectric dispersion) and the imaginary part (or dielectric loss) of the protein solution, σ is the electrical conductivity of the solution, and ε_0 is the vacuum permittivity (Figure 1b). To investigate the temperature effect on the collective vibration motions of protein and the protein−water interaction, we collected the dielectric response spectra at different temperatures between 5 and 55 °C. Figure 1c shows the dielectric response spectra for the 10 mM myoglobin solution at six selected temperatures.

The interaction between the megahertz-to-terahertz electromagnetic wave with biological solutions reveals the collective vibrational motions as well as the hydration structure and dynamics of hydrated biomolecules (Figure 1). The dielectric dispersion, $\varepsilon'(\nu)$, for both pure water and myoglobin solutions reduces with increasing frequency, and the values for myoglobin solutions are lower. The dielectric loss, $\varepsilon''(\nu)$, shows a complex behavior. The frequency of the main peak centered at ∼20 GHz appears in both water and myoglobin solutions, but the maximum for the myoglobin solutions is lower when compared with that of water. Taking a closer look at the megahertz to gigahertz frequencies, the dielectric loss of the myoglobin solutions is higher than that of water. Thus, the increase in the dielectric loss at megahertz to gigahertz frequencies of protein solutions is not expected from the bulk water relaxation process.

3.1. Dynamics and Structure of Hydration Shells. The interaction of electromagnetic waves with water molecules in aqueous solutions at megahertz to gigahertz frequencies reveals mechanisms of the reorientation dynamics of water. The alternating electrical fields of the electromagnetic waves rotate molecules with an electrical dipole moment. The spectroscopy (Figure 1) provides conclusive information on water dynamics in hydration layers (δ_1 and δ_2-relaxation) as well as in bulk water (γ-relaxation).[8,10,11]

To explore the dielectric response at the megahertz to gigahertz frequencies, it is sufficient to consider Debye-type relaxations. At the molecular level, the interaction between

https://doi.org/10.1021/acsomega.2c02843
ACS Omega 2022, 7, 22020−22031

water molecules and protein modifies the dynamics of water molecules. Water molecules in protein solutions can be divided into several specific types, named bulk water and loosely and tightly bound water.

$$\varepsilon^*(\nu) = \varepsilon_\infty + \frac{\Delta\varepsilon_{TB}}{1 + i2\pi\nu\tau_{TB}} + \frac{\Delta\varepsilon_{LB}}{1 + i2\pi\nu\tau_{LB}} + \frac{\Delta\varepsilon_D}{1 + i2\pi\nu\tau_D} \quad (3)$$

where $\Delta\varepsilon_{TB} = \varepsilon_S - \varepsilon_1$, $\Delta\varepsilon_{LB} = \varepsilon_1 - \varepsilon_2$ and $\Delta\varepsilon_D = \varepsilon_2 - \varepsilon_\infty$ are dielectric strengths of tightly bound, loosely bound, and bulk water, respectively, identified by individual Debye relaxation processes; and, τ_{TB}, τ_{LB}, and τ_D are the corresponding relaxation times. ε_∞ is the contribution to the total dielectric response from interactions at high frequencies. ε_S is the static permittivity of the solution. The reorientation motion of large molecules (β-relaxation) such as myoglobin with a molecular weight of ~17.0 kDa is typically in the submegahertz frequencies,[10,44] and is not investigated in this paper. The reorientation relaxation of bulk water, τ_D, in protein solutions and pure water at 25 °C has been well-characterized at 19.25 GHz or 8.27 ps.[29,45,46] The reorientation dynamics of water molecules at the interfacial area around myoglobin are complex and less understood. Typically, they form two main types of bound water, namely, loosely- and tightly bound water molecules. Tightly bound water molecules have a direct and strong contact to the protein surface (δ_1-relaxation). They cannot move easily and are considered to be an integral part of the protein. Water molecules having weak interactions with the protein, including some water molecules at the surface of the protein and outside the first hydration layer, are associated with the loosely bound water (δ_2-relaxation).

Employing this method, we fit the dielectric spectra including the real part $\varepsilon'(\nu)$ and the imaginary part $\varepsilon''(\nu)$ as a function of myoglobin concentration in solution and temperature to eq 3. The relaxation time at 25 °C for bulk water in solutions is similar to that obtained in pure water 8.15 ± 0.35 ps (19.53 GHz).[29,45,46] For the 10 mM myoglobin solution, two longer relaxation times of 36.9 ± 1.9 and 568.7 ± 28.5 ps of water molecules in hydration layers were identified for loosely- and tightly bound water, respectively, with retardation factors of about 4.5 and 70 compared with bulk water. The fitting to the Debye model provides dielectric strengths of $\Delta\tau_D$ = 52.67 ± 2.65, $\Delta\tau_{LB}$ = 8.04 ± 0.39, and $\Delta\tau_{TB}$ = 2.63 ± 0.14, corresponding to the contribution of bulk water, loosely-, and tightly bound water, respectively. The dielectric spectra provide average macroscopic properties of molecules in the solution involving bulk water and loosely and tightly bound water. The observed behavior is in line with earlier studies on solvated biomolecules reporting the heterogeneous dynamics of water molecules over a large time scale from subpicoseconds to nanoseconds.[20,21,32,47,48]

To extract the dielectric response originating from bound water molecules, we subtracted the dielectric strength of bulk water in the solution determined by the relaxation time, τ_D, and dielectric contribution,$\Delta\epsilon_D$, from the experimental data (Figure 2b). Obviously, contributions of bound water molecules can be identified by a superposition of several relaxation processes that can be associated with two types of water molecules in protein hydration layers. The fitting parameters for myoglobin solutions with different concentrations at 25 °C are provided in Table 1, and for the 10 mM myoglobin solution at different temperatures in Table 2.

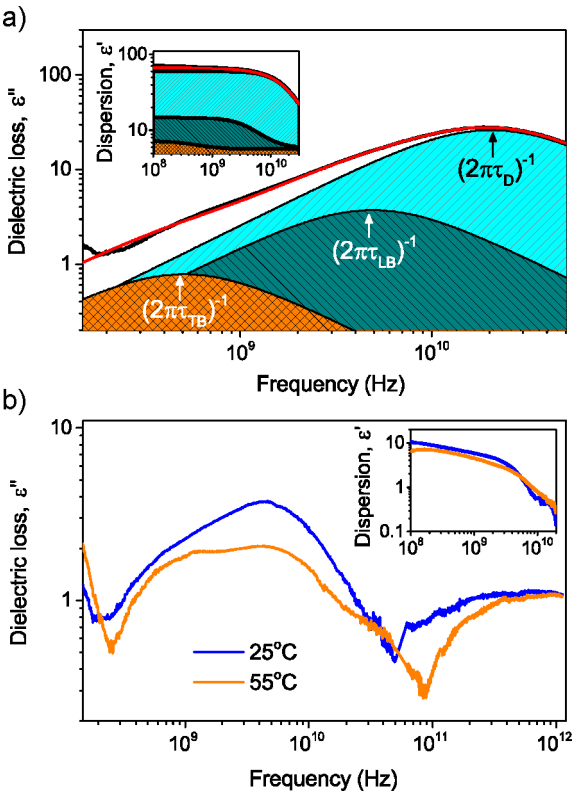

Figure 2. Dielectric response of the 10 mM myoglobin solution providing insight into the nature of hydration water at the molecular level. (a) Dielectric loss and dispersion (inset) spectra exhibit the cooperative relaxation dynamics of water molecules in the solution. The spectra are deconvoluted into three Debye elements, elucidating the contributions from the loosely bound (τ_{LB}), tightly bound (τ_{TB}), and bulk (τ_D) water in the solution. The red curves are fits to the dielectric spectra based on three Debye elements. (b) Dielectric loss and dispersion (inset) spectra for hydrated myoglobin are extracted at 25 and 55 °C, in which the bulk water contribution is subtracted.

The dielectric response of aqueous protein solutions provides information of the hydration dynamics and structure of water molecules around myoglobin. The dielectric contribution as well as the relaxation time as a function of myoglobin concentration in solution extracted from experimental data are demonstrated in Figure 3. The relaxation times for loosely (τ_{LB}) and tightly (τ_{TB}) bound water are shown within experimental uncertainty to be 36.8 ± 1.8 and 569.4 ± 28.5 ps, respectively, over the range of myoglobin concentration we have studied here (Figure 3a). The contribution of the dielectric strength for loosely bound ($\Delta\tau_{LB}$) and tightly bound *$\Delta\tau_{TB}$) water increases with a tendency to saturate at solutions with a high myoglobin concentration (Figure 3b). However, the dielectric amplitude of bulk water in solution, $\Delta\tau_D$, decreases monotonically with increasing myoglobin concentration (Figure 3c). The increase in the dielectric strength of bound water indicates that a higher number of water molecules are affected by protein when the concentration of myoglobin in solution increases. The lowering of the dielectric amplitude of bulk water is connected to water molecules in hydration shells, which are kinetically slowed down. Water molecules in hydration shells do not involve to the dynamics of bulk water, thus lowering the contribution to

https://doi.org/10.1021/acsomega.2c02843
ACS Omega 2022, 7, 22020−22031

Table 1. Relaxation Time (τ_i) and Dielectric Strength ($\Delta\varepsilon_i$) of the Dielectric Response, and Electrical Conductivity (σ) of Myoglobin Solutions at 25 °C, As Well As the Estimated Hydration Number (N_{hyd})[a]

c (mM)	τ_D (ps)	τ_{LB} (ps)	τ_{TB} (ps)	$\Delta\tau_D$	$\Delta\tau_{LB}$	$\Delta\tau_{TB}$	σ (S m^{-1})	N_{hyd}
1.00	8.26	37.1	576.8	71.25	0.97	0.55	0.13	1042
2.00	8.17	37.3	568.4	69.11	2.33	0.74	0.24	1014
3.25	8.24	36.4	568.2	66.50	3.54	0.95	0.31	989
5.00	8.05	36.9	567.6	63.00	4.93	1.55	0.37	976
7.50	8.23	36.2	566.1	58.86	6.11	1.95	0.40	957
10.0	7.88	36.3	569.3	52.67	8.04	2.63	0.46	941
15.0	8.15	37.5	564.4	43.28	9.76	3.33	0.51	840

[a]The errors for fitting parameters were less than 5%.

Table 2. Relaxation Time (τ_i) and Dielectric Strength ($\Delta\varepsilon_i$) of the Dielectric Response Collected from the 10 mM Myoglobin Solution at Different Temperatures[a]

T (°C)	τ_D (ps)	τ_{LB} (ps)	τ_{TB} (ps)	$\Delta\varepsilon_D$	$\Delta\varepsilon_{LB}$	$\Delta\varepsilon_{TB}$	N_{hyd}
5	14.9	42.6	636.9	57.04	11.12	1.76	1031
15	10.9	39.2	584.3	54.65	9.79	2.16	975
25	8.3	36.3	569.3	52.67	8.04	2.63	941
35	6.6	34.0	545.9	51.07	6.45	2.78	912
45	5.3	32.0	525.3	48.61	5.40	3.18	899
55	4.3	30.2	500.4	46.78	4.22	3.01	866

[a]The errors for fitting parameters were less than 5%.

the dielectric response of bulk water. In addition, the decrease in the dielectric strength of protein solutions also originates from the replacement of strongly absorbing water molecules by low absorbing protein molecules, reducing the absorption of aqueous solutions.

The presence of myoglobin in an aqueous solution modifies the dynamics of adjacent water molecules. The dielectric amplitude of bulk water in the myoglobin solutions can be used to estimate the number of water molecules in hydration shells. As mentioned before, water molecules considered as bulk water in the myoglobin solution relax with the time constant of τ_D. If all of the water molecules in the myoglobin solution are considered to be bulk water, the dielectric strength of these water molecules can be determined from the volume of water added to the solution, which corresponds to the "ideal bulk water", (blue line, Figure 3c). Nevertheless, in the myoglobin solutions, the dielectric amplitude of actual bulk water, $\Delta\varepsilon_D$, derived from fitting the experimental data to the Debye model (eq 3) is lower than the dielectric response of the "ideal bulk water" (Figure 3c). The difference increases considerably at high concentration of myoglobin in solution. This behavior indicates that in protein solution, all water molecules do not take part in the orientational relaxation of bulk water. A remarkable fraction of water is bound directly or indirectly to myoglobin via hydrogen bonding. These bound water molecules relax via longer relaxation times as compared to τ_D. The difference between dielectric strengths of the actual bulk water in the solution and the "ideal bulk water" yields the information of the "hydration effect" (Figure 3c). Thus, the number of "slow" water molecules per myoglobin or the "hydration number" can be determined as

$$N_{hyd}(c_{Mb}) = \frac{c_w - \frac{\Delta\varepsilon_w}{\Delta\varepsilon_{pure}} c_{pure}}{c_{Mb}} \quad (4)$$

where c_{pure} = 55.35 M is the molarity of pure water, $\Delta\varepsilon_{pure}$ is the dielectric strength of pure water, c_w is the water

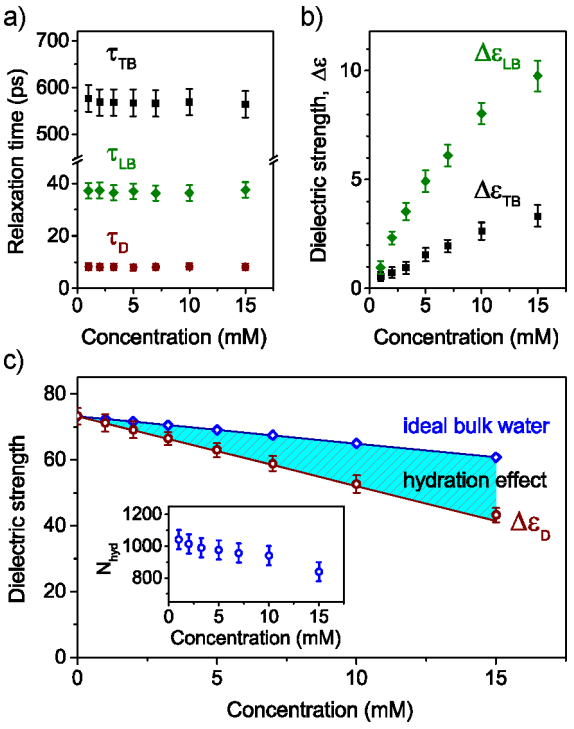

Figure 3. Dielectric response of relaxation processes in the megahertz to gigahertz frequency region indicating the existence of multiple relaxation processes in aqueous myoglobin solutions. (a) Reorientation relaxation times of loosely bound (τ_{LB}), tightly bound (τ_{TB}), and bulk (τ_D) water remain the same with different protein concentrations. (b) Dielectric strengths of relaxation processes of loosely and tightly bound water increase with protein concentration. (c) Dielectric strength of bulk water, $\Delta\varepsilon_D$, in aqueous myoglobin solutions monotonically decreases with the concentration. A difference between dielectric strengths of the "ideal bulk water" (blue line), under an assumption of all water relaxing via Δ_D mode, and bulk water in the protein solutions provides the information of the hydration effect. (inset) The hydration number, N_{hyd}, is an estimation of the number of water molecules per myoglobin that do not participate in bulk water relaxation.

concentration, c_{Mb} is the myoglobin concentration, and $\Delta\varepsilon_w$ is the dielectric strength of bulk water in the solution. Using the above approach, the number of water molecules, N_{hyd}, affected by the presence of a myoglobin molecule can be estimated of 1014 ± 50 in a 2 mM myoglobin solution. The value is slightly lower in solutions with high myoglobin concentration (Figure 3c, inset).

The hydration characteristics are consistent with the hydration properties of proteins where water molecules are kinetically affected by the protein's surface.[7,8,10] A minor

https://doi.org/10.1021/acsomega.2c02843
ACS Omega 2022, 7, 22020−22031

change in the hydration number with concentration is observed in the inset of Figure 3c. For low myoglobin concentration solutions, myoglobin molecules are well separated from each other, and the hydration dynamics is likely to be driven solely by myoglobin−water interactions. With increasing myoglobin concentration, the intermolecular distance between myoglobin molecules starts to decrease, and partial overlapping of hydration layers occurs in these solutions. A minor decrease in the hydration number in high myoglobin concentration solutions ensures that the overlapping of hydration layers is not taking effect extensively at the concentrations studied here.

MD simulations provide further information regarding the water distribution around proteins, including the structure and dynamics of water in hydration layers. The number of hydration water molecules in the loosely and tightly bound layers, respectively, is determined by calculating the number of water molecules involved in hydrogen bond to the protein surface, and within the bound hydration layers of the protein (approximately within the peak of the second layer of the water−protein radial distribution function).[49,50] MD simulations were performed over the same temperature range as the experiments.

To investigate the activity of water and myoglobin in aqueous solutions, the temperature dependence of the dielectric response for the 10 mM myoglobin solution was performed (Figure 1c) at 5, 15, 25, 35, 45, and 55 °C. As shown, when the temperature reduces, the dielectric spectra shift toward lower frequency. Fitting parameters of experimental results to eq 3 at different temperatures are presented in Figure 4. The reorientation relaxation times of water molecules in solutions become faster at higher temperature (Figure 4a). The dielectric strengths corresponding to the "ideal bulk water" in the solution were estimated with the above assumption that all water molecules relax with the τ_D relaxation mode at the individual temperature (Figure 4c). The dielectric strengths of the "ideal bulk water" as well as bulk water in myoglobin solutions decrease monotonically with increasing temperature. This behavior is consistent with the increased orientational correlation times (slower dynamics) when the temperature of the solution is lower, or the thermal fluctuation is reduced at lower temperature as reported in case of conventional molecular liquids.[51]

The number of water molecules affected by the myoglobin surface depends on the temperature of the environment. The difference between the dielectric strengths of the "ideal bulk water" and bulk water in the myoglobin solution increases at lower temperatures (Figure 4c). This indicates that the "hydration effect" increases with decreasing temperature as a result of which more water molecules become a part of the hydration shells. The hydration number at different temperatures was estimated similarly as described earlier. The hydration number decreases with increasing temperature (inset in Figure 4c). The observed trend can be explained by the concept of "Debye screening length" or simply "Debye length".[52] The Debye length is a measure of length-scale up to which electrostatic effect of a charged entity persists in a solvent medium. It has been reported previously that the Debye length increases with a decrease in temperature in the case of ionic liquids.[53,54] The observed response was attributed to a decrease in thermal fluctuations of the charged entities in the solution. At lower temperatures, the Debye length for myoglobin molecules increases and suppresses thermal

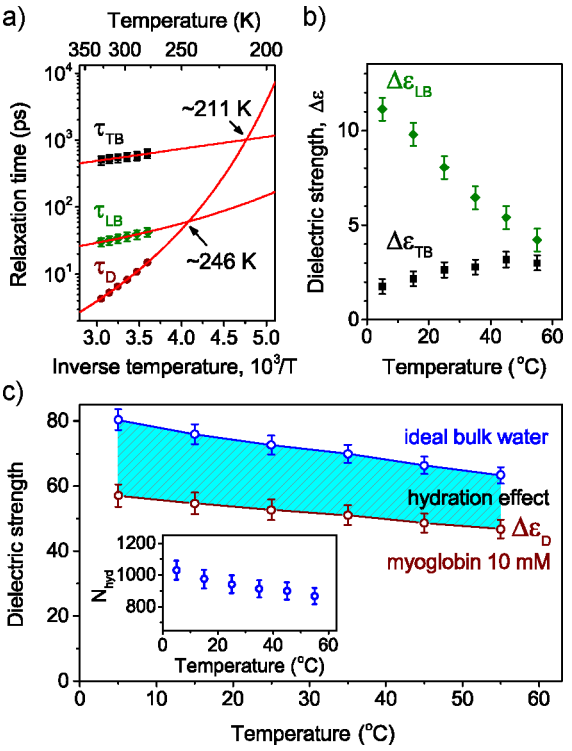

Figure 4. Dielectric response of relaxation processes of the 10 mM myoglobin solution in the megahertz to gigahertz frequency region depending on the temperature. (a) Reorientation relaxation times on a logarithmic scale of loosely bound (τ_{LB}), tightly bound (τ_{TB}), and bulk (τ_D) water increase with reducing temperature. (b) Dielectric strengths of relaxation processes of tightly and loosely bound water decrease with increasing temperature. (c) Dielectric strength of bulk water, $\Delta\tau_D$, in aqueous protein solutions monotonically decreases with increasing temperature. A difference between dielectric strengths of the "ideal bulk water" (blue circles) and bulk water in protein solutions provides the information on the hydration effect. (inset) The hydration number, N_{hyd}, is an estimation of the number of water molecules per myoglobin that do not participate in bulk water relaxation as a function of temperature.

fluctuation of myoglobin. This leads to a higher number of water molecules in the solution kinetically influenced at lower temperature. As a result, the effective hydration numbers increase at lower temperature. A significant increase in the dielectric strength has been observed for the loosely bound water, and a minor decrease in the dielectric strength of the tightly bound water molecules has been detected (Figure 4b). Overall, the increase in the bound water amplitudes can be attributed to the increased hydration effect at low temperatures.

3.2. Glass Transition Temperature of Hydration Water. To understand the coupling between the dynamics of a protein and its surrounding water, it is important to investigate the water dynamics as a function of temperature, especially in the low-temperature regime. It has come across that, unlike bulk water, hydration water does not crystallize even when the temperature is well below the crystal homogeneous nucleation temperature, $T_h \sim 235$ K, at ambient pressure.[14] However, the mechanisms governing the slowing down of hydration water are currently a matter of stimulating debate.[13,17,55−59] The dynamics of cold and hydrated proteins resembles the characteristics of glass formers, which are enslaved by the bulk solvent (γ-relaxation) and the first

https://doi.org/10.1021/acsomega.2c02843
ACS Omega 2022, 7, 22020−22031

hydration shell (δ_1-relaxation or referred to the Johari–Goldstein β-relaxation in the glass-physics community),[11,60,61] rather than the protein dynamical transition.[13] The γ-relaxation manipulates the shape of the protein, following a Vogel–Fulcher–Tammann (VFT)[62] function which has a non-Arrhenius behavior at higher temperatures. The δ_1-relaxation drives protein motions, exhibiting an Arrhenius relation at low temperature.[11,17] Recently, there has been experimental support that a liquid–liquid transition for water exists in supercooled water ∼180–220 K,[16−18,62] because glassy water is known to occur in two forms with different density. Connected to this proposed transition is a dynamical crossover, where the fragile behavior at high temperature (a non-Arrhenius temperature dependence of the γ-relaxation time) would change to the strong at low-temperature behavior (an Arrhenius temperature dependence of the δ_1-relaxation time).

The temperature dependence of relaxation times of water in protein solution provides dynamical properties of hydrated protein.[63−65] We analyze the relaxation time of loosely and tightly bound and bulk water molecules as a function of temperature in myoglobin solutions by fitting the data to the VFT[62] equation (eq 5) or the Arrhenius-type relation[62] (eq 6)

$$\tau = \tau_0 \exp\left[\frac{BT_0}{(T - T_0)}\right] \quad (5)$$

$$\tau = \tau_0 \exp\left[\frac{U}{k_B T}\right] \quad (6)$$

where T is the absolute temperature of the solution, T_0 is the glass transition temperature where the relaxation time, τ, appears to diverge, τ_0 is the relaxation time extrapolated to infinity temperature, B is the deviation from the Arrhenius activation energy and related to fragility, and U is the activation energy describing the rotation dynamics.

The temperature dependence of the relaxation time of bulk water in this frequency range follows the VFT (non-Arrhenius) behavior. The best fit for the relaxation time as a function of temperature yields $\tau_0 = 0.12 \times 10^{-12}$, $B = 5.31$, and $T_0 = 132 \pm 11$ K (red curve in Figure 4a). The temperature value, T_0, for bulk water obtained here is similar to reported values in the literature of ∼136 K for the glass transition temperature of water using various water mixtures at temperature down to 100 K.[45,66−68] Similarly, the temperature dependence of the dynamics of loosely bound water is well described by the VFT-type relation. The best fit for the relaxation time of the loosely bound water has been obtained as $\tau_0 = 9.24 \times 10^{-12}$, $B = 2.51$, and $T_0 = 105 \pm 11$ K. This suggests that the dynamics of loosely bound water molecules having a weak interaction with the protein surface follows the same glass transition behavior as bulk water. The glass transition temperature for the loosely bound water is lower and the value is closer to that of bulk water. From the extrapolation of the two VFT fitting curves, we find a crossover temperature for the loosely bound and bulk water at ∼246 K.

The complex interactions between protein and water have induced a strong distortion of the hydrogen bonding network. This indicates that the cooperative relaxation process of water has been affected strongly by the surface of the protein, forming a tightly bound water layer around the protein in myoglobin solutions. MD simulations indicate that water molecules directly hydrogen bonded to the protein constitute the vast majority of the tightly bound water molecules, as further discussed below. The temperature dependence of the relaxation time of tightly bound water follows the Arrhenius-type relation. We obtain best fits for the temperature dependence of the relaxation time for tightly bound water with $\tau_0 = 142.6 \times 10^{-12}$, $U/k_B = 412 \pm 29$. Because the relaxation process is not expected to participate in the glass transition of water, this observation supports the point that the process is originated from the first layer of hydration water. The extrapolation of fitting curves of the bulk water and the tightly bound water shows a crossing at 211 K. This value is similar to previous observations of ∼220 K for the fragile-to-strong dynamic crossover (non-Arrhenius to Arrhenius behavior transition) collected at the supercooled liquids for the γ- and δ_1-relaxation processes, corresponding to the relaxation of bulk and tightly bound water, respectively.[13,17,55,69] The results are consistent with calorimetric study,[69] broadband dielectric spectroscopy,[13,55] neutron scattering experiments,[16,17] and computational methods.[5,20,23,47,70] It is noted that bound water molecules in hydration shells are not localized with respect to their distance from protein surface and a significant dynamic exchange between bound and bulk water molecules takes place, as reported by Bagchi et al.[5,20,23,47,70] The theoretical models show a distinct behavior of hydrogen bond exchange of bulk water and tightly bound water molecules. The time constants as well as activation energy obtained here are in line with theoretical estimation based on the dynamic exchange of bulk and bound water in protein solutions.[70]

The temperature dependence of the dielectric strength of the tightly bound water, $\Delta\tau_{TB}$, shows an opposite behavior to those observed for the loosely bound and bulk water. The dielectric strength of the tightly bound water increases with increasing temperature and the trend cannot be interpreted as the γ-relaxation of the bulk water. These water molecules located at the interface between the protein and the water have reorientational motion with small angle (thermal activation).[71] Thus, the relaxation process involving localized molecule motions depends on temperature. The monotonic increase of the dielectric strength with temperature originates from the strong coupling of water molecules to protein surface by hydrogen boding. The behavior has been observed for confined water molecules when mixing water with hydrophilic solutes and in nanometer spaces.[58,61,71] The water molecules have a strong interaction with myoglobin's surface, and relax with Arrhenius temperature dependence. They become an integral part of the protein.

The reorientational dynamics of water within the hydration shell, evaluated using different cutoff distances from the myoglobin surface, at 15 °C are shown in Figure 5a. As can be seen, water molecules closest to the protein surface are the primary contributors to the slowest dynamics within the autocorrelation function (ACF). The protein–water radial distribution function (RDF) shows two well-defined peaks around 2.75 and 3.5 Å, as well as an outer, less-defined hydration shell peaking around 4.5 Å (Figure 5a, inset). For the MD analysis, tightly bound water molecules are defined as those that are directly hydrogen-bonded to the protein. Figure 5b shows the reorientation correlation functions for hydration water molecules at 5, 35, and 55 °C. As expected, the reorientational dynamics generally accelerate with temperature. However, the reorientational lifetime of molecules hydrogen-bonded to the protein (tightly bound water, black line, Figure

https://doi.org/10.1021/acsomega.2c02843
ACS Omega 2022, 7, 22020−22031

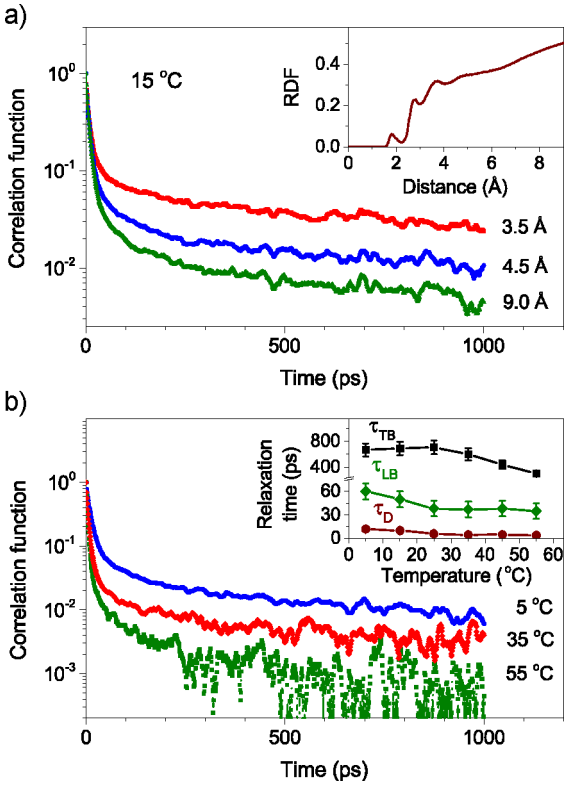

Figure 5. Dipole reorientation autocorrelation functions (ACFs) from MD simulations for water in the protein solution containing multiple exponential-decay components. (a) ACFs at 15 °C evaluated for water molecules within 3.5, 4.5, and 9.0 Å distance from the protein surface indicate three different dynamics including loosely-, tightly bound and bulk water. The protein−water radial distribution function (upper inset) shows three hydration layers peaked at ∼2.75, 3.5, and 4.5 Å. Slower dynamics are observed for water closer to the protein surface. b) The ACFs for water molecules within 4.5 Å from the protein surface display the dynamics of hydration water at different temperatures (5, 35, and 55 °C). The variation of the water relaxation times (lower inset) as a function of temperature has been investigated.

5b, inset) is found to hold steady or increase slightly with temperatures up to 25 °C, and then decrease at higher temperatures. Meanwhile, the reorientational lifetimes of loosely bound water decrease with temperature, following a similar trend as the dynamics of bulk water.

3.3. Collective Vibrations of Hydrated Proteins. At terahertz frequencies, the electromagnetic waves interact with collective vibrational motions of protein in solution, including inter- and intramolecular motions of molecular chains as well as hydration layers. In myoglobin solutions, water molecules around myoglobin form loosely- and tightly bound hydration layers (Figure 2). Water molecules in the tightly bound hydration layer have direct and strong contacts with the myoglobin surface, primarily in the form of hydrogen bonds. They become an essential part of the protein and cannot move easily.[7,10,28] Terahertz dielectric spectra of hydrated myoglobin in aqueous solutions reflect low-frequency vibrations, involving backbone and sidechains collective motions as well as water−myoglobin interactions. With high precision and simultaneous measurements of the absorption coefficient and refractive index of aqueous myoglobin solutions, we are able to adequately analyze the collective vibrational modes of hydrated myoglobin and the number of water molecules in the tightly bound hydration layer.

As a result of a heterogeneous system, myoglobin solutions can be described as a mixture of hydrated myoglobin and water, in which each component has its own dielectric property, $\varepsilon^*_{\mathrm{hMb}}$ and $\varepsilon^*_{\mathrm{wat}}$, respectively. The combination of the complex dielectric response of water and hydrated myoglobin results in the dielectric response of the solution, $\varepsilon^*_{\mathrm{sol}}$, which is determined from experimental results of absorption coefficient, $\alpha(\nu)$ and refractive index, $n(\nu)$.[10,72,73] The size of hydrated myoglobin is orders of magnitude smaller than the wavelength of probing electromagnetic waves, so the composite systems can be approximated as an effective homogeneous medium. Several effective-medium theory (EMT) models[73−76] have been proposed for systems based on physical characteristics of the individual components. Given the high dielectric contrast between water and myoglobin molecules, the choice of EMT models requires special attention. The Bruggeman model,[72−74] suitable for a high permittivity contrast and anisotropic medium, was used in the form

$$\varepsilon^*_{\mathrm{hMb}}(\nu) = \frac{2\varepsilon^{*\,2}_{\mathrm{sol}} + (3f_{\mathrm{h}} - 2)\varepsilon^*_{\mathrm{sol}}\varepsilon^*_{\mathrm{wat}}}{(3f_{\mathrm{h}} - 1)\varepsilon^*_{\mathrm{sol}} + \varepsilon^*_{\mathrm{sol}}} \tag{7}$$

where f_{h} is the volume fraction of hydrated myoglobin in the solution. The model equally treats the high and low concentration limits of solutes under specific considerations. First, a portion of water molecules absorbed in the tightly bound hydration shell of a myoglobin is considered to be an integral part of the myoglobin molecule in the aqueous solution. These water molecules located in the first hydration layer have a strong and direct contact to the surface of myoglobin and are kinetically retarded compared to that of the rest of water molecules. Second, myoglobin molecules were approximated as spherical macromolecules with radius, R_{Mb}. They are enclosed by the tightly bound water molecules, and the water molecules are imbedded within an average thickness of d from the surface of myoglobin. The volume fraction of hydrated myoglobin can be represented as $f_{\mathrm{hMb}} = (N_{\mathrm{Mb}}/V)(4\pi/3)(R_{\mathrm{Mb}} + d)^3$, where N_{Mb}/V is the myoglobin concentration in the aqueous solution. The estimation requires that the dielectric loss falls to zero at zero frequency.[73] Finally, molecular properties of the tightly bound water molecules were assumed to be similar to bulk water, but their dynamics are kinetically retarded.

Applying the Bruggeman effective-medium analysis, we estimated the dielectric response and the number of water molecules in the tightly bound hydration layer of a hydrated myoglobin (Figure 6a). Broad spectra of the dielectric loss of hydrated myoglobin at different temperatures have been identified with a peak intensity around 1 THz. The broad spectra of hydrated protein have been observed in the literature[3,10] and correlated with protein activities.[10] The number of water molecules in the tightly bound hydration layer considered as an integral part of myoglobin is found to be of ∼200−225 per myoglobin at most temperatures, comprising less than one water layer from the myoglobin surface. Note that these water molecules are not kinetically frozen; however, they are highly enslaved to myoglobin collective motions. The estimation of the number of water molecules in the tightly bound layer shows a local minimum at a temperature of around 20−30 °C (Figure 6c).

https://doi.org/10.1021/acsomega.2c02843
ACS Omega 2022, 7, 22020−22031

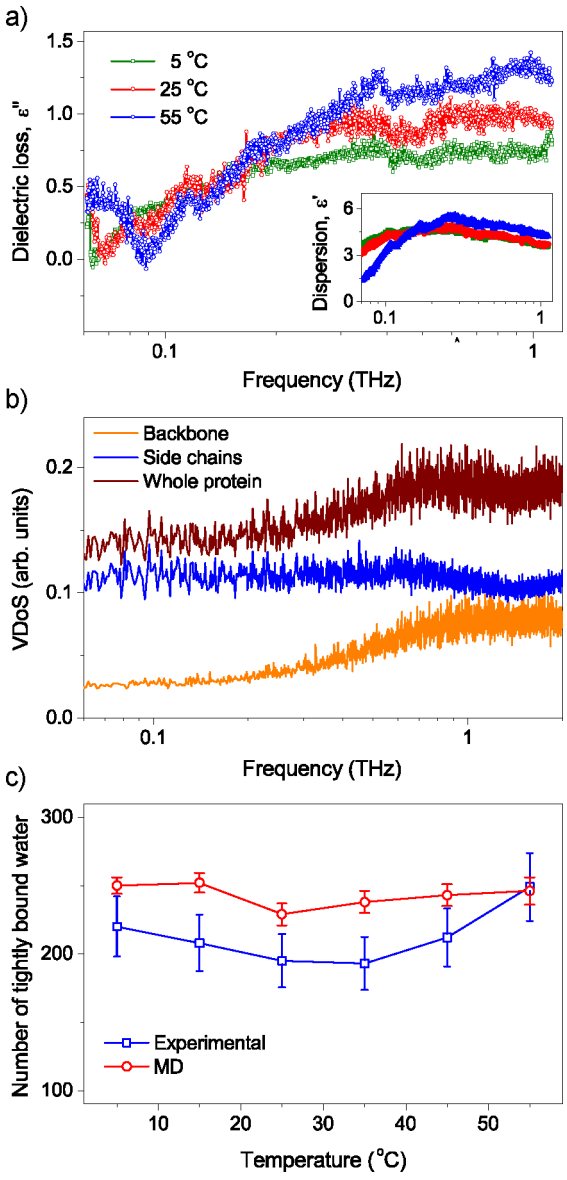

Figure 6. Dielectric response of hydrated myoglobin, uncovering collective motions of myoglobin in the aqueous environment. (a) Dielectric loss and dispersion (inset) of hydrated myoglobin are estimated using the Bruggeman effective-medium approximation at different temperatures for the 10 mM myoglobin solution. (b) VDoS of aqueous myoglobin at 25 °C. (c) Number of water molecules in the tightly bound hydration layer is a part of the hydrated myoglobin protein. MD results show the number of protein−water hydrogen bonds.

To maintain the specific three-dimensional conformations for biological function, proteins must have structural stability at the physiological temperature. The flexibility of the protein and the hydration water allows the structure to change rapidly with high sensitivity to regulatory signals. Thus, the preference for myoglobin stability should be a balance between stability and flexibility of structure rather than the maximum stability. Water plays an important role for the structural stability and lability of hydrated proteins. The total number of water molecules affected by the presence of myoglobin, including the loosely and tightly bound water or the hydration number, reduces with increasing temperature (Figure 3c). However, the number of tightly bound water molecules, which is an integral part of myoglobin exhibits a local minimum at 20−30 °C (Figure 6c), indicating an optimum for myoglobin function at the physiological temperature.

The dynamics of hydrated myoglobin strongly depend on temperature. At higher temperature, a larger collective motion has been expected. As can be seen from Figure 6a, the amplitude of the dielectric loss spectra of hydrated myoglobin increases from 5 to 55 °C, indicating a higher activity of myoglobin at higher temperature. To establish an adequate picture for hydrated myoglobin at the molecular level, we conducted MD simulations to investigate the hydration structure and dynamics of myoglobin. The purpose was to combine computational results to experimental dielectric responses and, thus, provide a microscopic insight into the collective motions and hydration dynamics of myoglobin in solution. We compute the vibrational density of states (VDoS) of hydrated myoglobin (in aqueous solution), characterizing the collective vibrational modes of side chains and backbone. The results of aqueous myoglobin solution at 25 °C are shown in Figure 6b. The VDoS spectrum of the side chains has its peak intensity at a frequency around 0.7 THz, whereas that of the backbone spectrum has a slightly broader peak at about 1 THz. As a result, the VDoS spectrum of myoglobin chain exhibits a maximum at ∼1 THz. The MD simulations are in good agreement with the experimental results.

4. CONCLUSIONS

We have employed broad-band dielectric spectroscopy from megahertz to terahertz frequencies to map out the dynamics of protein and water in aqueous solutions in the range from femto- to nanosecond, providing insights into the flexibility and stability of protein in aqueous environments under physiological conditions. The dielectric spectroscopy in the megahertz to gigahertz region indicates three main relaxation polarization processes of water in myoglobin solutions, including the tightly bound, loosely bound, and bulk water with reorientation times of 550, ∼40, and 8 ps, respectively, at room temperature. The relaxation dynamics become faster at elevated temperature. The temperature dependence of the relaxation time of loosely bound and bulk water molecules follows non-Arrhenius behavior with extrapolated glass transition temperatures of 105 and 132 K, respectively. However, the relaxation time for the tightly bound water molecules as a function of temperature obeys the Arrhenius type. Following the extrapolations of these behavior, we realized that there are two dynamic crossover points at the low-temperature regime of the water in protein solutions at 211 and 246 K.

The collective motions and hydration structure of myoglobin depend strongly on the temperature. The amplitude of the dielectric loss spectra of hydrated myoglobin increases with temperature, indicating a higher activity of hydrated myoglobin at higher temperature. The total number of water molecules affected by the presence of a myoglobin molecule (hydration number) has been estimated to be ∼1000, including both loosely and tightly bound water. In higher myoglobin concentration solutions, hydration shells start to overlap, resulting in a decrease in the hydration number. Combining molecular dynamic simulations and the terahertz spectroscopy results, we are able to estimate the number of tightly bound water molecules, which is about 200−250 molecules per protein, as well as the collective vibrational modes of hydrated myoglobin proteins as a function of

https://doi.org/10.1021/acsomega.2c02843
ACS Omega 2022, 7, 22020−22031

temperature. MD simulations yield results in excellent agreement with experiments, showing ∼230 water molecules directly hydrogen bonded to the surface of a myoglobin around physiological temperature. Furthermore, the MD simulations indicate that the predominant contribution to the dielectric spectra at the terahertz region originates from large-scale collective motions of hydrated myoglobin proteins.

■ ASSOCIATED CONTENT

Supporting Information

The Supporting Information is available free of charge at https://pubs.acs.org/doi/10.1021/acsomega.2c02843.

Dielectric response of myoglobin solutions at 25 °C for water, 2, 5, 10, and 15 mM myoglobin solutions, and the dieletric response of the 10 mM myoglobin solutions at difference temperatures (PDF)

■ AUTHOR INFORMATION

Corresponding Author

Nguyen Q. Vinh − *Department of Physics and Center for Soft Matter and Biological Physics, Virginia Tech, Blacksburg, Virginia 24061, United States; Department of Mechanical Engineering, Virginia Tech, Blacksburg, Virginia 24061, United States;* orcid.org/0000-0002-3071-1722; Phone: 540-231-3158; Email: vinh@vt.edu

Authors

Luan C. Doan − *Department of Physics and Center for Soft Matter and Biological Physics, Virginia Tech, Blacksburg, Virginia 24061, United States; Department of Mechanical Engineering, Virginia Tech, Blacksburg, Virginia 24061, United States*

Jayangika N. Dahanayake − *Department of Chemistry, Faculty of Science, University of Kelaniya, Kelaniya 11600, Sri Lanka*

Katie R. Mitchell-Koch − *Department of Chemistry, Wichita State University, Wichita, Kansas 67260, United States*

Abhishek K. Singh − *Department of Physics and Center for Soft Matter and Biological Physics, Virginia Tech, Blacksburg, Virginia 24061, United States*

Complete contact information is available at: https://pubs.acs.org/10.1021/acsomega.2c02843

Notes

The authors declare no competing financial interest.

■ ACKNOWLEDGMENTS

The authors gratefully acknowledge financial support by the National Science Foundation CHE-1665157 (N.Q.V. and K.R.M.) and Air Force Office of Scientific Research under award FA9550-18-1-0263 (N.Q.V.).

■ REFERENCES

(1) Grimaldo, M.; Roosen-Runge, F.; Zhang, F.; Schreiber, F.; Seydel, T. Dynamics of proteins in solution. *Q. Rev. Biophys.* **2019**, *52*, No. e7.

(2) Somero, G. N. Proteins and Temperature. *Annu. Rev. Physiol.* **1995**, *57*, 43−68.

(3) Markelz, A. G.; Roitberg, A.; Heilweil, E. J. Pulsed terahertz spectroscopy of DNA, bovine serum albumin and collagen between 0.1 and 2.0 THz. *Chem. Phys. Lett.* **2000**, *320*, 42−48.

(4) Daniel, R. M.; Dunn, R. V.; Finney, J. L.; Smith, J. C. The Role of Dynamics in Enzyme Activity. *Annu. Rev. Biophys. Biomol. Struct.* **2003**, *32*, 69−92.

(5) Nandi, N.; Bhattacharyya, K.; Bagchi, B. Dielectric relaxation and solvation dynamics of water in complex chemical and biological systems. *Chem. Rev.* **2000**, *100*, 2013−2045.

(6) Ebbinghaus, S.; Kim, S. J.; Heyden, M.; Yu, X.; Gruebele, M.; Leitner, D. M.; Havenith, M. Protein sequence- and pH-dependent hydration probed by terahertz spectroscopy. *J. Am. Chem. Soc.* **2008**, *130*, 2374−2375.

(7) Vinh, N. Q.; Allen, S. J.; Plaxco, K. W. Dielectric Spectroscopy of Proteins as a Quantitative Experimental Test of Computational Models of Their Low-Frequency Harmonic Motions. *J. Am. Chem. Soc.* **2011**, *133*, 8942−8947.

(8) Cametti, C.; Marchetti, S.; Gambi, C. M. C.; Onori, G. Dielectric Relaxation Spectroscopy of Lysozyme Aqueous Solutions: Analysis of the Delta-Dispersion and the Contribution of the Hydration Water. *J. Phys. Chem. B* **2011**, *115*, 7144−7153.

(9) Barends, T. R. M.; Foucar, L.; Ardevol, A.; Nass, K.; Aquila, A.; Botha, S.; Doak, R. B.; Falahati, K.; Hartmann, E.; Hilpert, M.; Heinz, M.; Hoffmann, M. C.; Kofinger, J.; Koglin, J. E.; Kovacsova, G.; Liang, M.; Milathianaki, D.; Lemke, H. T.; Reinstein, J.; Roome, C. M.; Shoeman, R. L.; Williams, G. J.; Burghardt, I.; Hummer, G.; Boutet, S.; Schlichting, I. Direct observation of ultrafast collective motions in CO myoglobin upon ligand dissociation. *Science* **2015**, *350*, 445−450.

(10) Charkhesht, A.; Regmi, C. K.; Mitchell-Koch, K. R.; Cheng, S.; Vinh, N. Q. High-Precision Megahertz-to-Terahertz Dielectric Spectroscopy of Protein Collective Motions and Hydration Dynamics. *J. Phys. Chem. B* **2018**, *122*, 6341−6350.

(11) Wolf, M.; Emmert, S.; Gulich, R.; Lunkenheimer, P.; Loidl, A. Dynamics of Protein Hydration Water. *Phys. Rev. E* **2015**, *92*, 032727.

(12) Fenimore, P. W.; Frauenfelder, H.; McMahon, B. H.; Young, R. D. Bulk-solvent and hydration-shell fluctuations, similar to alpha- and beta-fluctuations in glasses, control protein motions and functions. *Proc. Natl. Acad. Sci. U.S.A.* **2004**, *101*, 14408−14413.

(13) Frauenfelder, H.; Chen, G.; Berendzen, J.; Fenimore, P. W.; Jansson, H.; McMahon, B. H.; Stroe, I. R.; Swenson, J.; Young, R. D. A unified model of protein dynamics. *Proc. Natl. Acad. Sci. U.S.A.* **2009**, *106*, 5129−5134.

(14) Rupley, J. A.; Careri, G. Protein Hydration and Function. *Adv. Protein Chem.* **1991**, *41*, 37−172.

(15) Lagi, M.; Chu, X. Q.; Kim, C. S.; Mallamace, F.; Baglioni, P.; Chen, S. H. The low-temperature dynamic crossover phenomenon in protein hydration water: Simulations vs experiments. *J. Phys. Chem. B* **2008**, *112*, 1571−1575.

(16) Chen, S. H.; Liu, L.; Fratini, E.; Baglioni, P.; Faraone, A.; Mamontov, E. Observation of fragile-to-strong dynamic crossover in protein hydration water. *Proc. Natl. Acad. Sci. U.S.A.* **2006**, *103*, 9012−9016.

(17) Swenson, J.; Jansson, H.; Bergman, R. Relaxation processes in supercooled confined water and implications for protein dynamics. *Phys. Rev. Lett.* **2006**, *96*, 247802.

(18) Kumar, P.; Franzese, G.; Stanley, H. E. Predictions of dynamic behavior under pressure for two scenarios to explain water anomalies. *Phys. Rev. Lett.* **2008**, *100*, 105701.

(19) Sterpone, F.; Melchionna, S. Thermophilic proteins: insight and perspective from in silico experiments. *Chem. Soc. Rev.* **2012**, *41*, 1665−1676.

(20) Mukherjee, S.; Mondal, S.; Acharya, S.; Bagchi, B. Tug-of-War between Internal and External Frictions and Viscosity Dependence of Rate in Biological Reactions. *Phys. Rev. Lett.* **2022**, *128*, 108101.

(21) Duboue-Dijon, E.; Fogarty, A. C.; Hynes, J. T.; Laage, D. Dynamical Disorder in the DNA Hydration Shell. *J. Am. Chem. Soc.* **2016**, *138*, 7610−7620.

(22) Mondal, S.; Mukherjee, S.; Bagchi, B. Protein Hydration Dynamics: Much Ado about Nothing? *J. Phys. Chem. Lett.* **2017**, *8*, 4878−4882.

(23) Mukherjee, S.; Mondal, S.; Bagchi, B. Mechanism of Solvent Control of Protein Dynamics. *Phys. Rev. Lett.* **2019**, *122*, 058101.

(24) Leitner, D. M.; Pandey, H. D.; Reid, K. M. Energy Transport across Interfaces in Biomolecular Systems. *J. Phys. Chem. B* **2019**, *123*, 9507−9524.
(25) Mondal, S.; Mukherjee, S.; Bagchi, B. Origin of diverse time scales in the protein hydration layer solvation dynamics: A simulation study. *J. Chem. Phys.* **2017**, *147*, 154901.
(26) George, D. K.; Charkhesht, A.; Vinh, N. Q. New terahertz dielectric spectroscopy for the study of aqueous solutions. *Rev. Sci. Instrum.* **2015**, *86*, 123105.
(27) Charkhesht, A.; Lou, D.; Sindle, B.; Wen, C. Y.; Cheng, S. F.; Vinh, N. Q. Insights into Hydration Dynamics and Cooperative Interactions in Glycerol-Water Mixtures by Terahertz Dielectric Spectroscopy. *J. Phys. Chem. B* **2019**, *123*, 8791−8799.
(28) George, D. K.; Charkhesht, A.; Hull, O. A.; Mishra, A.; Capelluto, D. G. S.; Mitchell-Koch, K. R.; Vinh, N. Q. New Insights into the Dynamics of Zwitterionic Micelles and Their Hydration Waters by Gigahertz-to-Terahertz Dielectric Spectroscopy. *J. Phys. Chem. B* **2016**, *120*, 10757−10767.
(29) Vinh, N. Q.; Sherwin, M. S.; Allen, S. J.; George, D. K.; Rahmani, A. J.; Plaxco, K. W. High-Precision Gigahertz-to-Terahertz Spectroscopy of Aqueous Salt Solutions as a Probe of the Femtosecond-to-Picosecond Dynamics of Liquid Water. *J. Chem. Phys.* **2015**, *142*, 164502.
(30) Maurya, D.; Charkhesht, A.; Nayak, S. K.; Sun, F. C.; George, D.; Pramanick, A.; Kang, M. G.; Song, H. C.; Alexander, M. M.; Lou, D.; Khodaparast, G. A.; Alpay, S. P.; Vinh, N. Q.; Priya, S. Soft phonon mode dynamics in Aurivillius-type structures. *Phys. Rev. B* **2017**, *96*, 134114.
(31) Singh, A. K.; Wen, C. Y.; Cheng, S. F.; Vinh, N. Q. Long-range DNA-water interactions. *Biophys. J.* **2021**, *120*, 4966−4979.
(32) Reid, K. M.; Singh, A. K.; Bikash, C. R.; Wei, J.; Tal-Gan, Y.; Vinh, N. Q.; Leitner, D. M. The origin and impact of bound water around intrinsically disordered proteins. *Biophys. J.* **2022**, *121*, 540−551.
(33) Kachalova, G. S.; Popov, A. N.; Bartunik, H. D. A steric mechanism for inhibition of CO binding to heme proteins. *Science* **1999**, *284*, 473−476.
(34) Dahanayake, J. N.; Gautam, D. N.; Verma, R.; Mitchell-Koch, K. R. To keep or not to keep? the question of crystallographic waters for enzyme simulations in organic solvent. *Mol. Simulat* **2016**, *42*, 1001−1013.
(35) Abraham, M. J.; Murtola, T.; Schulz, R.; Pall, S.; Smith, J. C.; Hess, B.; Lindahl, E. GROMACS: High performance molecular simulations through multi-level parallelism from laptops to supercomputers. *SoftwareX* **2015**, *1−2*, 19−25.
(36) Huang, J.; MacKerell, A. D. CHARMM36 all-atom additive protein force field: Validation based on comparison to NMR data. *J. Comput. Chem.* **2013**, *34*, 2135−2145.
(37) Berendsen, H. J. C.; Grigera, J. R.; Straatsma, T. P. The Missing Term in Effective Pair Potentials. *J. Phys. Chem.* **1987**, *91*, 6269−6271.
(38) Xu, H. F.; Stern, H. A.; Berne, B. J. Can water polarizability be ignored in hydrogen bond kinetics? *J. Phys. Chem. B* **2002**, *106*, 2054−2060.
(39) Hess, B.; Bekker, H.; Berendsen, H. J. C.; Fraaije, J. G. E. M. LINCS: A linear constraint solver for molecular simulations. *J. Comput. Chem.* **1997**, *18*, 1463−1472.
(40) Darden, T.; York, D.; Pedersen, L. Particle Mesh Ewald - an N.Log(N) Method for Ewald Sums in Large Systems. *J. Chem. Phys.* **1993**, *98*, 10089−10092.
(41) Bussi, G.; Donadio, D.; Parrinello, M. Canonical Sampling Through Velocity Rescaling. *J. Chem. Phys.* **2007**, *126*, 014101−7.
(42) Berendsen, H. J. C.; Postma, J. P. M.; Vangunsteren, W. F.; Dinola, A.; Haak, J. R. Molecular-Dynamics with Coupling to an External Bath. *J. Chem. Phys.* **1984**, *81*, 3684−3690.
(43) Evans, D. J.; Holian, B. L. The Nose-Hoover Thermostat. *J. Chem. Phys.* **1985**, *83*, 4069−4074.
(44) Oleinikova, A.; Sasisanker, P.; Weingartner, H. What Can Really Be Learned from Dielectric Spectroscopy of Protein Solutions? A Case Study of Ribonuclease A. *J. Phys. Chem. B* **2004**, *108*, 8467−8474.
(45) Ellison, W. J. Permittivity of Pure Water, at Standard Atmospheric Pressure, over the Frequency Range 0−25 THz and the Temperature Range 0−100 Degrees C. *J. Phys. Chem. Ref. Data* **2007**, *36*, 1−18.
(46) Buchner, R.; Hefter, G. Interactions and Dynamics in Electrolyte Solutions by Dielectric Spectroscopy. *Phys. Chem. Chem. Phys.* **2009**, *11*, 8984−8999.
(47) Mukherjee, S.; Mondal, S.; Acharya, S.; Bagchi, B. DNA Solvation Dynamics. *J. Phys. Chem. B* **2018**, *122*, 11743−11761.
(48) Ebbinghaus, S.; Kim, S. J.; Heyden, M.; Yu, X.; Heugen, U.; Gruebele, M.; Leitner, D. M.; Havenith, M. An extended dynamical hydration shell around proteins. *Proc. Natl. Acad. Sci. U.S.A.* **2007**, *104*, 20749−20752.
(49) Dahanayake, J. N.; Mitchell-Koch, K. R. Entropy connects water structure and dynamics in protein hydration layer. *Phys. Chem. Chem. Phys.* **2018**, *20*, 14765−14777.
(50) Dahanayake, J. N.; Shahryari, E.; Roberts, K. M.; Heikes, M. E.; Kasireddy, C.; Mitchell-Koch, K. R. Protein Solvent Shell Structure Provides Rapid Analysis of Hydration Dynamics. *J. Chem. Inf Model* **2019**, *59*, 2407−2422.
(51) Harrison, G. *Dynamic Properties of Supercooled Liquids*; Academic Press, 1976.
(52) Debye, P.; Hückel, E. The theory of electrolytes. I. Freezing point depres-sion and related phenomena [Zur Theorie der Elektrolyte. I. Gefrierpunktserniedrigung und verwandte Erscheinungen]. *Phys. Z.* **1923**, *24*, 185−206.
(53) Gebbie, M. A.; Dobbs, H. A.; Valtiner, M.; Israelachvili, J. N. Long-range electrostatic screening in ionic liquids. *Proc. Natl. Acad. Sci. U.S.A.* **2015**, *112*, 7432−7437.
(54) Lee, A. A.; Perez-Martinez, C. S.; Smith, A. M.; Perkin, S. Scaling analysis of the screening length in concentrated electrolytes. *Phys. Rev. Lett.* **2017**, *119*, 026002.
(55) Mazza, M. G.; Stokely, K.; Pagnotta, S. E.; Bruni, F.; Stanley, H. E.; Franzese, G. More than one dynamic crossover in protein hydration water. *Proc. Natl. Acad. Sci. U.S.A.* **2011**, *108*, 19873−19878.
(56) Kuo, Y. H.; Chiang, Y. W. Slow Dynamics around a Protein and Its Coupling to Solvent. *ACS Cent. Sci.* **2018**, *4*, 645−655.
(57) Pawlus, S.; Khodadadi, S.; Sokolov, A. P. Conductivity in hydrated proteins: No signs of the fragile-to-strong crossover. *Phys. Rev. Lett.* **2008**, *100*, 108103.
(58) Capaccioli, S.; Ngai, K. L.; Ancherbak, S.; Bertoldo, M.; Ciampalini, G.; Thayyil, M. S.; Wang, L. M. The JG beta-relaxation in water and impact on the dynamics of aqueous mixtures and hydrated biomolecules. *J. Chem. Phys.* **2019**, *151*, 034504.
(59) Taschin, A.; Bartolini, P.; Eramo, R.; Righini, R.; Torre, R. Evidence of two distinct local structures of water from ambient to supercooled conditions. *Nat. Commun.* **2013**, *4*, 2401.
(60) Johari, G. P.; Goldstein, M. Viscous Liquids and Glass Transition.2. Secondary Relaxations in Glasses of Rigid Molecules. *J. Chem. Phys.* **1970**, *53*, 2372.
(61) Swenson, J.; Cerveny, S. Dynamics of deeply supercooled interfacial water. *J. Phys-Condens Mat* **2015**, *27*, 033102.
(62) Mallamace, F.; Branca, C.; Corsaro, C.; Leone, N.; Spooren, J.; Chen, S. H.; Stanley, H. E. Transport properties of glass-forming liquids suggest that dynamic crossover temperature is as important as the glass transition temperature. *Proc. Natl. Acad. Sci. U.S.A.* **2010**, *107*, 22457−22462.
(63) Nakanishi, M.; Sokolov, A. P. Protein dynamics in a broad frequency range: Dielectric spectroscopy studies. *J. Non-Cryst. Solids* **2015**, *407*, 478−485.
(64) Shinyashiki, N.; Yamamoto, W.; Yokoyama, A.; Yoshinari, T.; Yagihara, S.; Kita, R.; Ngai, K. L.; Capaccioli, S. Glass Transitions in Aqueous Solutions of Protein (Bovine Serum Albumin). *J. Phys. Chem. B* **2009**, *113*, 14448−14456.

https://doi.org/10.1021/acsomega.2c02843
ACS Omega 2022, 7, 22020−22031

(65) Ringe, D.; Petsko, G. A. The 'glass transition' in protein dynamics: what it is, why it occurs, and how to exploit it. *Biophys. Chem.* **2003**, *105*, 667−680.
(66) Cerveny, S.; Schwartz, G. A.; Bergman, R.; Swenson, J. Glass transition and relaxation processes in supercooled water. *Phys. Rev. Lett.* **2004**, *93*, 245702.
(67) Amann-Winkel, K.; Gainaru, C.; Handle, P. H.; Seidl, M.; Nelson, H.; Bohmer, R.; Loerting, T. Water's second glass transition. *Proc. Natl. Acad. Sci. U.S.A.* **2013**, *110*, 17720−17725.
(68) Gallo, P.; Amann-Winkel, K.; Angell, C. A.; Anisimov, M. A.; Caupin, F.; Chakravarty, C.; Lascaris, E.; Loerting, T.; Panagiotopoulos, A. Z.; Russo, J.; et al. Water: A Tale of Two Liquids. *Chem. Rev.* **2016**, *116*, 7463−7500.
(69) Jansson, H.; Bergman, R.; Swenson, J. Role of Solvent for the Dynamics and the Glass Transition of Proteins. *J. Phys. Chem. B* **2011**, *115*, 4099−4109.
(70) Nandi, N.; Bagchi, B. Dielectric relaxation of biological water. *J. Phys. Chem. B* **1997**, *101*, 10954−10961.
(71) Ngai, K. L.; Paluch, M. Classification of secondary relaxation in glass-formers based on dynamic properties. *J. Chem. Phys.* **2004**, *120*, 857−873.
(72) Hernandez-Cardoso, G. G.; Singh, A. K.; Castro-Camus, E. Empirical comparison between effective medium theory models for the dielectric response of biological tissue at terahertz frequencies. *Appl. Opt.* **2020**, *59*, D6−D11.
(73) Choy, T. C. *Effective Medium Theory: Principle and Applications*; Clarendon Press, 1999.
(74) Bruggeman, D. A. G. Berechnung Verschiedener Physikalischer Konstanten von Heterogenen Substanzen. *Ann. Phys. Leipzig* **1935**, *416*, 636−664.
(75) Garnett, J. C. M. Colours in Metal Glasses and in Metallic Films. *Philos. Trans. R. Soc. London, Ser. A* **1904**, *203*, 385−420.
(76) Hanai, T. Theory of the Dielectric Dispersion due to the Interfacial Polarization and its Application to Emulsions. *Colloid Polym. Sci.* **1960**, *171*, 23−31.

https://doi.org/10.1021/acsomega.2c02843
ACS Omega 2022, 7, 22020−22031